# Volitional Contractility Assessment of Plantar Flexors by Using Non-invasive Neuromuscular Measurements

Qiang Zhang, Ashwin Iyer, Kang Kim*, and Nitin Sharma*

***Abstract*—This paper investigates an ultrasound (US) imaging-based methodology to assess the contraction levels of plantar flexors quantitatively. Echogenicity derived from US imaging at different anatomical depths, including both lateral gastrocnemius (LGS) and soleus (SOL) muscles, is used for the prediction of the volitional isometric plantar flexion moment. Synchronous measurements, including a plantar flexion torque signal, a surface electromyography (sEMG) signal, and US imaging of both LGS and SOL muscles, are collected. Four feature sets, including sole sEMG, sole LGS echogenicity, sole SOL echogenicity, and their fusion, are used to train a Gaussian process regression (GPR) model and predict plantar flexion torque. The experimental results on four non-disabled participants show that the torque prediction accuracy is improved significantly by using the LGS or SOL echogenicity signal than using the sEMG signal. However, there is no significant improvement by using the fused feature compared to sole LGS or SOL echogenicity. The findings imply that using US imaging-derived signals improves the accuracy of predicting volitional effort on human plantar flexors. Potentially, US imaging can be used as a new sensing modality to measure or predict human lower limb motion intent in clinical rehabilitation devices.**

## I. Introduction

The human ankle joint produces a large burst of "push-off" mechanical power in the late stance phase of walking. A reduction in the "push-off" force, due to neurological disorders or injuries, leads to a considerably poorer energy economy during walking [1]. For people with multiple sclerosis, those recovering from stroke [2], and individuals with ankle arthrodesis or arthroplasty [3], the peak push-off power during ankle plantar flexion is reduced by more than half. This ankle dysfunction severely impedes their normal activities of daily living, especially for walking, running, jumping, and dancing. The recent therapy techniques to improve weakened plantar flexion function mainly focus on powered ankle exoskeletons [4], and functional electrical stimulation (FES) [5], [6]. Effectiveness of control strategies, such as assist-as-needed control, for operating these neurorehabilitation devices depends on determining voluntary plantar flexion torque. However, non-invasively measuring human limb joint torque remains a major challenge.

Surface electromyography (sEMG) is a widely-used non-invasive neuromuscular measurement for detecting voluntary human limb mechanical functions, e.g., joint moment [7], [8], angular position [9], and joint stiffness [10]. sEMG measures electrical potentials during muscle neurons firings, whose amplitude and frequency are positively related to the muscle contraction force [11]. The determination of correlation between sEMG signals and human limb mechanical functions can be categorized into neuromuscular model-based and model-free approaches. Lloyd et al. [12] examined if an EMG driven musculoskeletal model of the human knee could be used to predict knee torques, calculating using inverse dynamics under multiple contractile conditions. In [13], the authors developed a mathematical muscle model based on anatomical and physiological data to estimate joint torque solely from EMG. And joint stiffness was directly obtained by differentiation of this model analytically. In [14], the authors constructed a complete forward dynamics model (FDM) by using an artificial neural network that learned nonlinear functions, relating physiological recordings of EMG signals to joint trajectories. Zhang et al. [15] proposed to use a BP neural network to built the $m^{th}$ order nonlinear model between the sEMG signals and joints angles of human legs. Experimental results on both non-disabled people and spinal cord injury patients showed good performance on joint angles estimation. However, sEMG-based intent detection has several shortcomings, such as signal interference from adjunct muscles and an inability to measure the signal from deeply-located muscles [16].

Alternatively, ultrasound (US) imaging is another non-invasive method that avoids the shortcomings of sEMG by providing direct visualization of targeted skeletal muscle contractions. The most frequently used structural parameters from US images include: pennation angle (PA) [11], [17], fascicle length (FL) [18], and muscle thickness (MT) [19]. These parameters have also been studied to determine a mapping between US-derived structural parameters and joint

Qiang Zhang, Ashwin Iyer, and Nitin Sharma are with the UNC & NC State Joint Department of Biomedical Engineering, NC State University, Raleigh, NC, USA. (e-mail: qzhang25@ncsu.edu, aiyer3@ncsu.edu, and nsharm23@ncsu.edu).

Kang Kim is with the Department of Bioengineering, University of Pittsburgh School of Engineering, Pittsburgh, PA, USA. (e-mail: kangkim@upmc.edu). Kang Kim is also with the Center for Ultrasound Molecular Imaging and Therapeutics-Department of Medicine and Heart and Vascular Institute, University of Pittsburgh School of Medicine and University of Pittsburgh Medical Center, Pittsburgh, PA, USA. Kang Kim is also with the Department of Mechanical Engineering and Materials Science, University of Pittsburgh School of Engineering, Pittsburgh, PA, USA. Kang Kim is also with the McGowan Institute for Regenerative Medicine, University of Pittsburgh and University of Pittsburgh Medical Center, Pittsburgh, PA, USA. (*Co-corresponding authors: Kang Kim and Nitin Sharma)

This work was funded by NSF CAREER Award # 1750748.

mechanical functions, such as muscle force [20] and joint torque [21], [22]. In [23], five US-image-derived features of the superficial rectus femoris (RF) muscle were used to estimate the distal knee joint angle and velocity by using a regression-based machine learning approach. The authors in [24] used a contraction rate adaptive speckle tracking algorithm to detect the quadriceps contraction strain by using US imaging, which acted as an indicator of muscle fatigue due to FES. Our previous work [11] explored the superior ankle dorsiflexion torque prediction performance by combing US imaging-derived parameters and sEMG signal based on a modified Hill-type neuromuscular model. However, the majority of the studies used sole sEMG signals or US imaging-derived features to estimate human limb mechanical functions, and few studies have worked on the estimation impact by using the fusion of sEMG and US imaging. In addition, those structural parameters, including PA, FL, and MT, are usually off-line extracted, which impedes the online implementation. Also, the reliable performance of feature extraction algorithms depends on the image resolution and selection of the region of interest (ROI), which varies from trial to trial and person to person.

Compared to the structural parameters from US image, echogenicity covers more information in the ROI without depending too much on the image resolution. It is preferred for online implementation, although its physical and physiological relevance is unclear. Generally, echogenicity represents the brightness and darkness of the US image and is calculated by taking the mean gray-scale value of each pixel in the ROI. In this paper, we fuse echogenicity and sEMG signals to predict human plantar flexion torque. A Gaussian process regression (GPR) model uses the combined signals. Another advantage of GPR is its ability to overcome noise in neuromuscular measurements. Experimental results on four non-disabled participants are analyzed to evaluate the prediction performance by using the fused feature compared to the prediction by using sole echogenicity and sole sEMG signals with the GPR model.

## II. Methods

### A. Subjects

Institutional Review Board (IRB) at the University of Pittsburgh (IRB approval number: PRO18020072) approved this study. Four participants (Age: 24.5 $\pm$ 2.1 years old), without any neuromuscular disorders, were recruited in this study. Every participant signed an informed consent form before participating in the experiments.

### B. Experimental Protocol

The experimental setup for this study is illustrated in Fig. 1 (a), where each participant was seated on a chair with adjustable height and instructed to perform two separate experiment sets. The first experiment set was to determine the maximum voluntary isometric contraction (MVIC) during isometric plantar flexion for the posture shown in Fig. 1 (a). Participants were asked to achieve and maintain MVIC for 2 seconds and the maximum torque was recorded. The second experiment set was to collect continuous-time measurement data, including US imaging, sEMG signal, and plantar flexion torque. Participants were instructed to cyclically perform plantar flexion within a 11-second duration for three periods in each trial. The participants started in a relaxed state, then increased the plantar flexors contraction to MVIC, sustained at MVIC for around 1 second, and finally relaxed the plantar flexors. This procedure with three periods was repeated three times as three trials and a 2-minute rest period was provided between two successive trials to avoid muscle fatigue.

During the isometric plantar flexion, the participant's upper leg was held horizontally on the level chair seat by velcro straps to limit any knee and upper leg motion during the plantar flexion. The lower leg was kept perpendicular to the upper leg and the foot. The plantar flexors include medial gastrocnemius (MGS), lateral gastrocnemius (LGS), and soleus (SOL) muscles. Through physical and visual observation of how plantar flexors move during the isometric plantar flexion, a location 10 cm distal to the knee joint was chosen as the targeted region, where LGS and SOL muscles locate at superficial and deep locations. The region is shown as the yellow dashed line in Fig. 1 (a). A sEMG sensor (Bagnoli$^{TM}$ Desktop, DELSYS, MA, USA) was attached to the skin through double-sided tape to non-invasively measure the LGS's electrical signals during the plantar flexion. A clinical linear US transducer (L7.5SC Prodigy Probe, S-Sharp, Taiwan) was attached to the skin by a customized 3-D printed holder, as shown in Fig. 1 (b). The holder with 1 rotational degree of freedom (DOF) can rotate the transducer from cross-sectional direction to longitudinal direction, as shown in Fig. 1 (c). Thus, the holder can be adjusted to obtain a suitable transducer orientation for observing plantar flexors' structure at different depths, as shown in Fig. 1 (f). The elevation angle in between the holder base (attaching to the skin) and holder arm (stabilizing the US transducer) in Fig. 1 (b) was designed as a fixed angle of 90°, which implies that the US transducer was always kept perpendicular to the targeted tissue. Conductive US gel was applied between the skin and US transducer. Due to the placement of the US transducer (shown in Fig. 1 (d)), only the direction going through LGS and SOL can be imaged at different depths. The segmentation between LGS and SOL is participant-specific. As shown in Fig. 1 (f), the depth that ranges between 8 mm and 32 mm is the LGS muscle while the portion that ranges between 32 mm and 62 mm is the SOL muscle. A load cell platform in 1 (e), as used in [11] was used to measure the isometric plantar flexion torque by multiplying the force measurement from load cell and a constant moment arm (approximately 0.1 m).

### C. Data Acquisition and Processing

The measurements from load cell, sEMG, and US machine were synchronized and sampled at the same frequency by a real-time system in MATLAB/Simulink (R2012b, MathWorks, MA, USA). The signals from the load cell were processed by a signal conditioner (DRC-4710, OMEGA Engineering, CT, USA) and then collected by a data acquisition

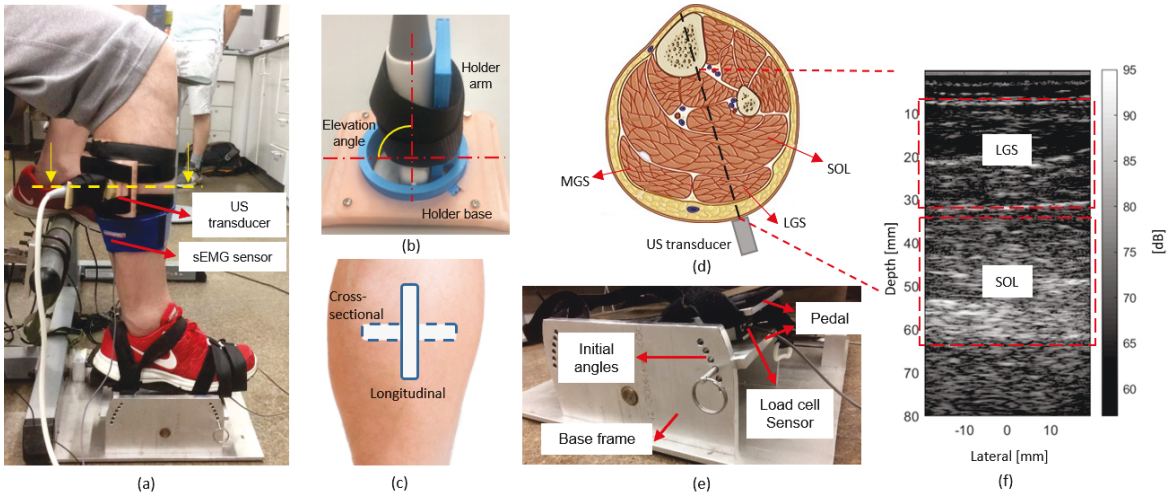


Figure 1. Experimental setup illustration for isometric plantar flexion.

board (DAQ, QPIDe Board, Quanser, Canada). The signals from the sEMG sensor were processed by an input module and a main amplifier (BagnoliTM Desktop, DELSYS, MA, USA) with an amplified gain 10 k, filtered to the bandwidth between 20 Hz and 450 Hz, and then collected by the DAQ. For the US machine, the pulse sequence (PS) mode was employed to image the muscles during isometric plantar flexion due to its ultrafast sampling rate characteristic. The synchronization of US imaging to load cell (sEMG) signal was guaranteed by designing a trigger sequence with 1000 Hz frequency and 5 % duty cycle in the Simulink real-time system. The first second of the 11 seconds was left blank to initialize the data collection procedure, and the three plantar flexion periods were finished within the remaining 10 seconds. All sensors were sampled at 1000 Hz.

The isometric plantar flexion torque time sequence was defined as $y^{(i)}$, ($i = 1, 2, ..., n$ represents the torque value at the $i^{th}$ sampling instant). The sEMG signals were processed by taking the moving root mean square (MRMS), which was detailed in our previous work [8], [11], and denoted as $x_0^{(i)}$. The raw data from US imaging were beamformed to gray-scaled US images offline in MATLAB, as shown in Fig. 1 (f). By direct observation, LGS and SOL were segmented in the two rectangular boxes. The echogenicity values of LGS and SOL, calculated by averaging the linearized decibel values (from 0 to 255) of all pixels in the corresponding ROIs, were denoted as $x_1^{(i)}$ and $x_2^{(i)}$.

### *D. Data Training, Prediction, and Statistical Analysis*

Gaussian process regression (GPR) has been widely applied to predict continuous quantities [25]. A GPR model is a non-parametric kernel-based probabilistic model. It defines a distribution over functions, and interface takes place directly in the functions space, which is known as the function-space view [25]. Each plantar flexion torque measurement $y^{(i)}$ can be thought of as related to an underlying function $g(x_j^{(i)})$, $j = 0, 1, 2$, and 3 with respect sEMG feature set, LGS echogenicity set, SOL echogenicity set, and fused feature set, and a Gaussian noise model is given as

$$y^{(i)} = g(x_j^{(i)}) + \mathcal{N}(0, \sigma_{jn}^2) \tag{1}$$

where $\sigma_{jn}^2$ is the variance for each neuromuscular signal. The purpose of regression is to search for the underlying function $g(x_j^{(i)})$.

A novel approach of folding the noise into the covariance function, as mentioned in [26], can be represented as a "squared exponential" choice

$$k(x_j^{(p)}, x_j^{(q)}) = \sigma_{jf}^2 e^{\frac{-\left(x_j^{(p)} - x_j^{(q)}\right)^2}{2l^2}} + \sigma_{jn}^2 \delta(x_j^{(p)}, x_j^{(q)}) \tag{2}$$

where $\sigma_{jf}^2$ is the maximum allowable covariance for each neuromuscular signal, $x_j^{(p)}$ and $x_j^{(q)}$ are the two sampled neuromuscular measurements at $p^{th}$ and $q^{th}$ sampling points, and $\delta(x_j^{(p)}, x_j^{(q)})$ is the Kronecker delta function. If $x_j^{(p)} \approx x_j^{(q)}$, then the first term of (2) approaches its maximum value, meaning $g(x_j^{(p)})$ is almost perfectly correlated with $g(x_j^{(q)})$. If $x_j^{(p)}$ is distant from $x_j^{(q)}$, the first term of (2) approaches to 0. In addition, the effect of this separation will depend on the length parameter, $l$.

The redefinition in (2) is equally suitable for the objective in this work, which is to predict the plantar flexion torque $y_j^*$ by using new neuromuscular measurement set $x_j^*$, based on the given $n-$dimensional plantar flexion torque measurement, $y$, and neuromuscular measurement set, $x_j$. In order to perform GPR, the covariance functions among all possible combinations of data from each neuromuscular measure are calculated, and the results are summarized into three matrices

$$K_j = \begin{bmatrix} k(x_j^{(1)}, x_j^{(1)}) & k(x_j^{(1)}, x_j^{(2)}) & \cdots & k(x_j^{(1)}, x_j^{(n)}) \\ k(x_j^{(2)}, x_j^{(1)}) & k(x_j^{(2)}, x_j^{(2)}) & \cdots & k(x_j^{(2)}, x_j^{(n)}) \\ \vdots & \vdots & \ddots & \vdots \\ k(x_j^{(n)}, x_j^{(1)}) & k(x_j^{(n)}, x_j^{(2)}) & \cdots & k(x_j^{(n)}, x_j^{(n)}) \end{bmatrix} \tag{3}$$

$$K_j^{*(m)} = \begin{bmatrix} k(x_j^{*(m)}, x_j^{(1)}) & \cdots & k(x_j^{*(m)}, x_j^{(n)}) \end{bmatrix} \tag{4}$$

$$K_j^{**(m)} = \left[k(x_j^{*(m)}, x_j^{*(m)})\right] \tag{5}$$

where $x_j^{*(m)}$, $m = 1, 2, 3...$, represents the new measurement set, which will be used in the prediction procedure.

Based on the key assumption of Gaussian process modeling that the data can be represented as a sample from a multivariate Gaussian distribution, we can derive that

$$\begin{bmatrix} y \\ y_j^{*(m)} \end{bmatrix} \sim \mathcal{N}\left(0, \begin{bmatrix} K_j & K_j^{*(m)T} \\ K_j^{*(m)} & K_j^{**(m)} \end{bmatrix}\right). \tag{6}$$

Furthermore, the conditional probability $p\left(y_j^{*(m)} \mid y\right)$ follows a Gaussian distribution, which can be given as

$$y_j^{*(m)} \mid y \sim \mathcal{N}\left(K_j^{*(m)} K_j^{-1} y,\, K_j^{**(m)} - K_j^{*(m)} K_j^{-1} K_j^{*(m)T}\right). \tag{7}$$

Therefore, the best estimate for the plantar flexion torque $y_j^{*(m)}$ is the mean value in the above Gaussian distribution

$$\bar{y}_j^{*(m)} = K_j^{*(m)} K_j^{-1} y \tag{8}$$

and the estimation uncertainty in the prediction procedure is considered as the variance in (7)

$$var(y_j^{*(m)}) = K_j^{**(m)} - K_j^{*(m)} K_j^{-1} K_j^{*(m)T}. \tag{9}$$

The outcomes from neuromuscular data acquisition and processing contain sEMG MRMS, LGS echogenicity, and SOL echogenicity from three repeated trials on every participant. The data were categorized into four feature sets, including sole sEMG MRMS feature, sole LGS echogenicity feature set, sole SOL echogenicity feature set, and fused feature set. In each trial, for every feature set, data of two plantar flexion periods were used for training and the remaining period was used for prediction based on leave-one-out cross validation principle through the GPR model.

One-way repeated-measure analysis of variance (ANOVA) followed by a Tukey's honestly significant difference test (Tukey's HSD) was applied to evaluate the prediction performance across four different feature sets on each participant. The significant difference level was chosen as $p < 0.05$.

## III. Results and Discussions

### A. Images of Plantar Flexors Contractility Change

As shown in Fig. 1 (f), the US image at the muscle's relaxed state was selected as the initial frame, and the same targeted ROIs in each new frame were compared with the ROIs in the initial frame. Figure 2 shows the linearized decibel value change of each pixel in both (a) LGS and (b) SOL at different volitional plantar flexion levels, including 0%, 25%, 50%, and 100% MVIC, each subplot corresponds to the change from previous contraction level (level-to-level change plot). By direct observation, the decibel values difference varies monotonically when the participants generate more plantar flexion torque, which implies that the decibel values change is highly correlated to the plantar flexion torque. In addition, with the increase of plantar flexion torque, the decibel value change rate of becomes lower, as shown the change from 25 % to 50 % MVIC and 50 % to 100 % MVIC compared to the change from rest to 25 % MVIC.

Table I
Correlation analysis results between echogenicity and torque, sEMG MRMS and torque on each participant.

| Participants | Trials | LGS -CC | SOL-CC | sEMG-CC |
|---|---|---|---|---|
| A1 | 1 | -0.958 | -0.945 | 0.926 |
| | 2 | -0.972 | -0.953 | 0.932 |
| | 3 | -0.974 | -0.956 | 0.928 |
| A2 | 1 | -0.925 | -0.956 | 0.892 |
| | 2 | -0.914 | -0.959 | 0.873 |
| | 3 | -0.919 | -0.923 | 0.759 |
| A3 | 1 | -0.939 | -0.923 | 0.903 |
| | 2 | -0.943 | -0.910 | 0.916 |
| | 3 | -0.957 | -0.927 | 0.900 |
| A4 | 1 | -0.937 | -0.937 | 0.755 |
| | 2 | -0.927 | -0.933 | 0.795 |
| | 3 | -0.928 | -0.932 | 0.761 |
| Average | | -0.941 | -0.938 | 0.862 |

### B. Correlation Analysis and Prediction Comparison

To facilitate the correlation between US imaging measures and plantar flexion torque, the two-dimensional image time sequence was converted to one-dimensional echogenicity time sequence for both LGS and SOL. Figure 3 shows the measurements of LGS echogenicity, SOL echogenicity, sEMG raw signal and sEMG MRMS signal, and the corresponding plantar flexion torque for the $1^{st}$ trial on participant A1. Visually, in this trial, sEMG MRMS is not as good as echogenicity to correlate with the plantar flexion torque. The correlation analysis among different neuromuscular measurements and plantar flexion torque was given by calculating the correlation coefficients (CCs), as given in Table I, where LGS-CC, SOL-CC, and sEMG-CC represent the correlation coefficients between LGS echogenicity and torque, between SOL echogenicity and torque, and between sEMG MRMS and torque, respectively. Except sEMG-CC in trial 3 on A2 and all trials on A4, all other CCs absolute values are higher than 0.8. The results also show that CC between echogenicity and torque is higher than CC between sEMG MRMS and torque.

The preliminary results from correlation analysis indicate that these neuromuscular measurements can be used to predict the ankle plantar flexion torque. As mentioned before, four feature sets are used to train the GPR model and predict plantar flexion torque by using new measured feature sets based on leave-one-out cross validation principle. The root mean square error (RMSE) between the predicted plantar flexion torque and torque measurement in each trial was calculated by taking the mean value of RMSE from cross validation process. To validate the performance of this GPR model for plantar flexion torque prediction, the prediction RMSE values across 3 trials on each participant (mean value $\pm$ standard deviation) were calculated and normalized to individual's MVIC, as shown in Fig 4. Results on all 4 participants show that the prediction RMSE value is significantly reduced by using either LGS echogenicity or SOL echogenicity compare to sEMG MRMS. Therefore, echogenicity from either of them can be selected to predict the ankle plantar flexion torque with higher accuracy than the sEMG signal. However, there is no significant difference between the prediction RMSE values by using LGS echogenicity and SOL

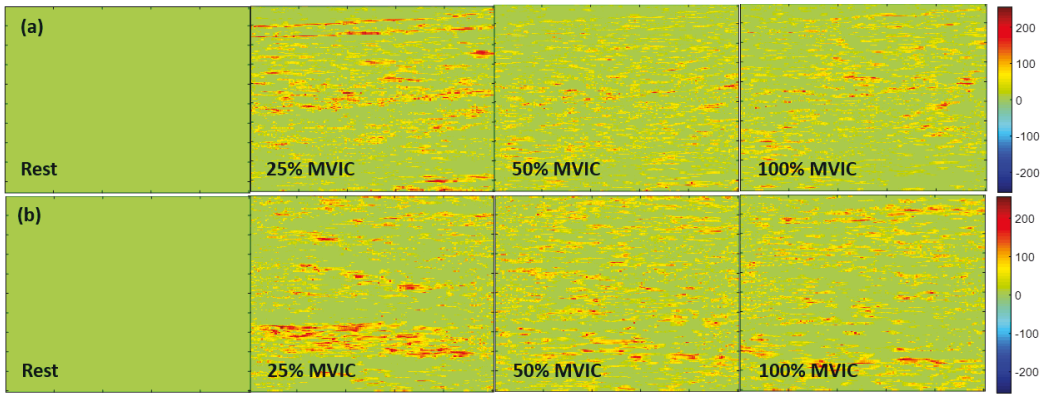


Figure 2. Plantar flexors contractility comparison among different contraction levels in the first volitional plantar flexion cycle of trial 1 on participant A1. (a) Images of the linearized decibel value change for each pixel on LGS. (b) Images of the linearized decibel value change for each pixel on SOL.

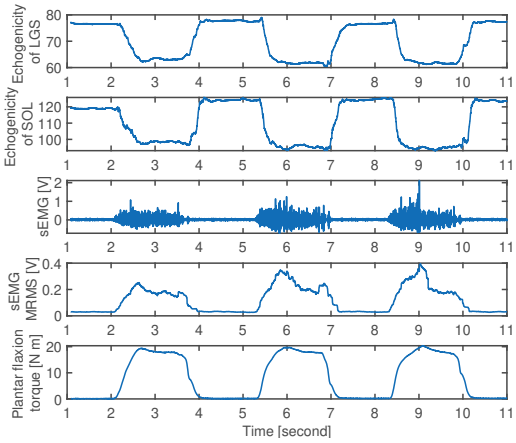


Figure 3. Measurements of plantar flexors' echogenicity from US images, raw and processed sEMG signals, and ankle plantar flexion torque on participant A1 in trial 1.

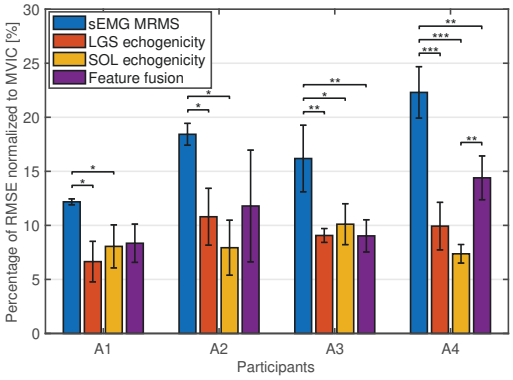


Figure 4. Prediction RMSE values normalized to MVIC on each participant by using 4 feature sets based on GPR model. ⋆, ⋆⋆, and ⋆⋆⋆ represent the significant difference level at $p < 0.05$, $p < 0.01$, and $p < 0.001$.

echogenicity. It implies that the proposed approach cannot differentiate contributions from LGS and SOL to plantar flexion torque. Furthermore, although the fused feature can reduce the prediction RMSE on four participants compared to sEMG MRMS, along with significant reduction on Participant A3 and A4, there is no evident reduction compared to LGS or SOL echogenicity, and there is even a significantly increased prediction RMSE on Participant A4. One possible reason is that the GPR model is very sensitive to the number of input variables sequence. While the fused feature set is prone to significantly reduce the training RMSE, it may cause overfitting for the GPR model and deteriorate the prediction performance.

### C. Discussion

The experimental results on 4 able-bodied participants verified our hypothesis that the US imaging would increase the ankle plantar flexion torque prediction accuracy compared to the sEMG signal. Across the 4 participants, compared to the sEMG signal, the averaged prediction RMSE normalized to each individual's MVIC was reduced 49.7 % by using LGS echogenicity and 55.7 % by using SOL echogenicity. However, by using GPR model, the fused feature set did not outperform sole LGS echogenicity or SOL echogenicity in the preliminary results. The results in Fig. 3 showed echogenicity for both LGS and SOL was negatively correlated to the torque, while the sEMG MRMS was positively correlated to the torque. A possible reason for the negative coorelation between echogenicity and plantar flexion torque is that the echogenicity is a physical property by which a tissue interacts with US waves. The brightness and darkness in Fig. 1 (f) represent the US reflection ability. Higher brightness means the reflection is higher, which is also called hyperechogenic, while the darkness is called hypoechogenic. It was indicated in [17] that the intramuscular fat, water, and fibrous tissue would increase the reflection ability while the isotropic muscle fibers would decrease the reflection ability. But with the increasing muscle contractions, those components are compressed and then the reflection ability reduces resulting in the decreased echogenicity. As shown in Fig. 3, the LGS and SOL echogenicity values at muscle relaxation state are around 78 and 120, respectively. In addition, the LGS and SOL echogenicity variation ranges are around 16 and 23, respectively. These difference between LGS and SOL echogenicity values indicates that overall SOL muscle contains more intramuscular fat, water, and fibrous

tissue than LGS. The preliminary results in this paper indicate that echogenicity in US images has a promising potential to non-invasively detect human plantar flexors' contraction force, which can be used as a feedback when implementing plantar flexion rehabilitation devices.

There are limitations in the current study. First, the setup of the current study was limited to a sitting state. The effects of different hip and knee initial positions on the proposed approach are unknown. Therefore, more experiments are needed to verify the prediction performance under extended hip extended and straight knee conditions. A single position-fixed ROI was defined as a rectangular shape for both LGS and SOL as shown in Fig. 1 (f), respectively, which may cause a problem of including other muscles due to the fact that muscle shape and thickness change as the muscle contracts. Also, more work is needed to investigate the proposed approach during walking. Finally, echogenicity from US imaging is sensitive to many factors, including pressure applied by the US transducer, orientation of the US transducer, and elevation angle between the US transducer and the targeted skin [27]. Effects of these factors were not considered in the study.

## IV. Conclusion

This paper proposed a non-invasive GPR-based approach that used echogenicity from US images to predict voluntary ankle plantar flexion torque. Multiple GPR models were respectively trained usingLGS echogenicity set, SOL echogenicity set, sEMG MRMS set, and fused feature set. The GPR models predicted new plantar flexion torque from the new measurements data sets. The results showed that the prediction RMSE was significantly reduced by using either LGS echogenicity or SOL echogenicity or fused feature set compared to sEMG MRMS. However, no significant difference in the reduction of the prediction RMSE was observed by using the fused feature set vis-a-vis the sole use of LGS echogenicity or SOL echogenicity set in the GPR model. The results imply US imaging as a potential sensing modality to detect human ankle volitional torque, which is vital for control of robotics-based devices, designed for both intact limbs and those with below the knee amputation.

## References


[1] P. H. Tzu-wei, K. A. Shorter, P. G. Adamczyk, and A. D. Kuo, "Mechanical and energetic consequences of reduced ankle plantar-flexion in human walking," *J. Exp. Biol.*, vol. 218, no. 22, pp. 3541–3550, 2015.

[2] D. Bregman, J. Harlaar, C. Meskers, and V. De Groot, "Spring-like ankle foot orthoses reduce the energy cost of walking by taking over ankle work," *Gait & posture*, vol. 35, no. 1, pp. 148–153, 2012.

[3] S. Singer, S. Klejman, E. Pinsker, J. Houck, and T. Daniels, "Ankle arthroplasty and ankle arthrodesis: gait analysis compared with normal controls," *JBJS*, vol. 95, no. 24, p. e191, 2013.

[4] D. P. Ferris, K. E. Gordon, G. S. Sawicki, and A. Peethambaran, "An improved powered ankle-foot orthosis using proportional myoelectric control," *Gait & Posture*, vol. 23, no. 4, pp. 425–428, 2006.

[5] R. van Swigchem, H. J. van Duijnhoven, J. den Boer, A. C. Geurts, and V. Weerdesteyn, "Effect of Peroneal Electrical Stimulation Versus an Ankle-Foot Orthosis on Obstacle Avoidance Ability in People With Stroke-Related Foot Drop," *Phys. Ther.*, vol. 92, no. 3, pp. 398–406, 2012.

[6] N. Kirsch, N. Alibeji, L. Fisher, C. Gregory, and N. Sharma, "A semi-active hybrid neuroprosthesis for restoring lower limb function in paraplegics," in *2014 IEEE EMBS*. IEEE, 2014, pp. 2557–2560.

[7] M. Sartori, D. Farina, and D. G. Lloyd, "Hybrid neuromusculoskeletal modeling to best track joint moments using a balance between muscle excitations derived from electromyograms and optimization," *J. Biomech.*, vol. 47, no. 15, pp. 3613–3621, 2014.

[8] Q. Zhang, Z. Sheng, F. Moore-Clingenpeel, K. Kim, and N. Sharma, "Ankle dorsiflexion strength monitoring by combining sonomyography and electromyography," in *2019 IEEE ICORR*. IEEE, 2019, pp. 240–245.

[9] J. Han, Q. Ding, A. Xiong, and X. Zhao, "A state-space emg model for the estimation of continuous joint movements," *IEEE Trans. Ind. Electron.*, vol. 62, no. 7, pp. 4267–4275, 2015.

[10] S. Pfeifer, H. Vallery, M. Hardegger, R. Riener, and E. J. Perreault, "Model-Based Estimation of Knee Stiffness," *IEEE Trans. Biomed. Eng.*, vol. 59, no. 9, pp. 2604–2612, 2012.

[11] Q. Zhang, K. Kim, and N. Sharma, "Prediction of Ankle Dorsiflexion Moment by Combined Ultrasound Sonography and Electromyography," *IEEE Trans. Neural Syst. Rehabil. Eng.*, vol. 28, no. 1, pp. 318–327, 2019.

[12] D. G. Lloyd and T. F. Besier, "An EMG-driven musculoskeletal model to estimate muscle forces and knee joint moments in vivo," *J. Biomech.*, vol. 36, no. 6, pp. 765–776, 2003.

[13] D. Shin, J. Kim, and Y. Koike, "A myokinetic arm model for estimating joint torque and stiffness from emg signals during maintained posture," *J. Neurophysiol.*, vol. 101, no. 1, pp. 387–401, 2009.

[14] Y. Koike and M. Kawato, "Estimation of dynamic joint torques and trajectory formation from surface electromyography signals using a neural network model," *Biol. Cybern.*, vol. 73, no. 4, pp. 291–300, 1995.

[15] F. Zhang, P. Li, Z.-G. Hou, Z. Lu, Y. Chen, Q. Li, and M. Tan, "semg-based continuous estimation of joint angles of human legs by using bp neural network," *Neurocomputing*, vol. 78, no. 1, pp. 139–148, 2012.

[16] L. J. Hargrove, K. Englehart, and B. Hudgins, "A comparison of surface and intramuscular myoelectric signal classification," *IEEE Trans. Biomed. Eng.*, vol. 54, no. 5, pp. 847–853, 2007.

[17] E. M. Strasser, T. Draskovits, M. Praschak, M. Quittan, and A. Graf, "Association between ultrasound measurements of muscle thickness, pennation angle, echogenicity and skeletal muscle strength in the elderly," *Age*, vol. 35, no. 6, pp. 2377–2388, 2013.

[18] A. Arampatzis, K. Karamanidis, S. Stafilidis, G. Morey-Klapsing, G. DeMonte, and G.-P. Brüggemann, "Effect of different ankle-and knee-joint positions on gastrocnemius medialis fascicle length and emg activity during isometric plantar flexion," *J. Biomech.*, vol. 39, no. 10, pp. 1891–1902, 2006.

[19] D. L. Damiano, L. A. Prosser, L. A. Curatalo, and K. E. Alter, "Muscle plasticity and ankle control after repetitive use of a functional electrical stimulation device for foot drop in cerebral palsy," *Neurorehabil. Neural Repair*, vol. 27, no. 3, pp. 200–207, 2013.

[20] P. Hodges, L. Pengel, R. Herbert, and S. Gandevia, "Measurement of muscle contraction with ultrasound imaging," *Muscle & Nerve*, vol. 27, no. 6, pp. 682–692, 2003.

[21] J. Shi, Y. P. Zheng, Q. H. Huang, and X. Chen, "Continuous monitoring of sonomyography, electromyography and torque generated by normal upper arm muscles during isometric contraction: Sonomyography assessment for arm muscles," *IEEE Trans. Biomed. Eng.*, vol. 55, no. 3, pp. 1191–1198, 2008.

[22] T. J. M. Dick, A. A. Biewener, and J. M. Wakeling, "Comparison of human gastrocnemius forces predicted by Hill-type muscle models and estimated from ultrasound images," *J. Exp. Biol.*, vol. 220, no. 9, pp. 1643–1653, 2017.

[23] M. H. Jahanandish, N. P. Fey, and K. Hoyt, "Lower-Limb Motion Estimation Using Ultrasound Imaging: A Framework For Assistive Device Control," *IEEE J. Biomed. Health Inform.*, pp. 1–10, 2019.

[24] Z. Sheng, N. Sharma, and K. Kim, "Quantitative assessment of changes in muscle contractility due to fatigue during nmes: An ultrasound imaging approach," *IEEE Trans. Biomed. Eng.*, 2019.

[25] C. K. Williams and C. E. Rasmussen, *Gaussian processes for machine learning*. MIT press Cambridge, MA, 2006, vol. 2, no. 3.

[26] M. Ebden *et al.*, "Gaussian processes for regression: A quick introduction," *The website of robotics research group in department on engineering science, University of Oxford*, vol. 91, pp. 424–436, 2008.

[27] B. Ihnatsenka and A. P. Boezaart, "Ultrasound: Basic understanding and learning the language," *Int. J. Shoulder Surg.*, vol. 4, no. 3, p. 55, 2010.